Sample Density Analysis and Optimization for NOAA's Airborne Snow Water Equivalent Surveys

Patrick D Didier

Advisor: Justine Blanford

Capstone Project Paper in Support of Master’s in Geographic Information Systems from Pennsylvania State University World Campus

Submitted: December 2016

Abstract

Since 1980, the National Oceanic and Atmospheric Administration (NOAA) has conducted airborne snow and soil moisture surveys using the attenuation of terrestrial gamma radiation from the top 20 cm of the soil. These surveys are used to provide critical snow-water equivalent data to water resource forecasters throughout the United States and parts of Canada. Due to limitations in the number of sensors, aircraft platforms, and trained mission crewmembers, it is imperative that these surveys are conducted as efficiently as possible. Over 30 years of survey sample density was investigated to determine if there existed any tendency to over-sample. The over-sampling candidate survey sample was reduced by 5, 10, and 25 percent using both SWE-dependent, and SWE-independent methods. Interpolated values were then compared against the measured values to develop sample errors for the sample-reduced survey. The lowest sample errors produced by these method exceeded the actual error inherent in the gamma collection method itself (1.0cm). This analysis led to the determination that over-sampling does not appear to be an issue within the airborne gamma detection program.

Background

The amount of snow on the ground has a significant impact to much of the population of the United States. In the western US, up to 85 percent of the runoff in the Colorado basin comes from snowmelt (Bales and Cline 2016). In the Upper Midwest, the historic flooding of the Red River of the North in 1997 caused an estimated $4 billion worth of damage, and resulted in the evacuation of over 55,000 residents in the United States and 28,000 rural residents in southern Canada (Todhunter 2001). Annual snow accumulation and corresponding melt has a significant impact on agriculture, transportation, and tourism (Adams, Houston, Weiher 2004). Accurate and timely measurement of the amount of water contained in the snowpack offers a significant cost benefit for the nation.

Since 1980, the National Weather Service has used airborne gamma detection to measure the amount of water in the snowpack for areas within the United States and Canada. These data are primarily used to predict snowmelt runoff by NOAA River Forecast Centers and Weather Forecast Offices. Additional stakeholders include the US Army Corps of Engineers (Moes 2011 and USACE 1992), and various other government and private entities.

Under gamma detection theory, the soil for a given area contains a set concentration of radioactive isotopes of uranium, thorium, and potassium. Within the top 20 cm of soil, radiation from these isotopes is emitted at a constant rate over time. An airborne-mounted detection system can sense this radiation when flown at sufficiently low altitude. Water, in any phase, attenuates the gamma radiation signal received by the sensor. Comparing the amount of radiation attenuation during dry conditions to the amount encountered under snow-covered conditions provides an estimate of snow-water equivalent (SWE). Field surveys have demonstrated the airborne gamma detection technique to be accurate to within 3.9% soil moisture (Jones and Carroll 1983), which amounts to less than 1 cm of snow-water equivalent.

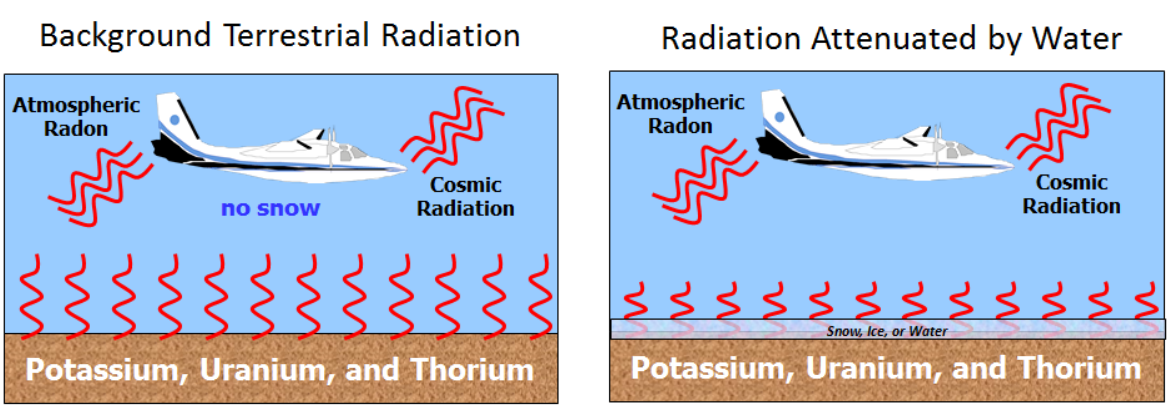

Figure 1. Radiation caused by naturally-occuring isotopes in the soil is attenuated due to the presence of water between the top 20 cm of soil and the airborne sensor.

Airborne Flight Line Data

The basic unit of data collection using the airborne gamma detection method is known as a "flight line". Each flight line represents a specific portion of the Earth's surface, and is created in such a manner that it can be flown in a fixed-wing aircraft at about 100-120 knots over the ground. These lines are flown at 500 feet above the ground, where the horizontal swath of the sensor is roughly 1000 feet. With the line being 10-15 miles long, this means that each flight line is representative of the mean areal snow-water-equivalent of an area of about 2.5 square miles (Figure 2-left).

In addition to the geospatial data that define each flight line, key background parameters are also contained within the flight line database. Each line has a unique gamma signature that includes the counts per minute for potassium, thorium and total counts, each normalized for 25 percent soil moisture. In addition to the average count rates, which remain stable from year to year, the background soil moisture for each flight line is updated annually to account for changing soil moisture conditions, based on either airborne measurements or model estimates. The remaining three columns contain the soil moisture value used in the SWE calculation, the method used to acquire soil moisture (estimate, fall survey measurement, or interpolation), and the date that the soil moisture value was last updated. (Figure 2-right).

When a flight line is flown, a single SWE measurement is recorded (Figure 3, Column 4), representing all water contained within the snow itself, ice on the ground, and any additional water in the top 20 cm of soil beyond what was estimated or measured for the background data. The single value that has been generated for each flight line represents the average SWE value for that entire flight line. Therefore, the SWE value for a line with a high degree of spatial variability within the line itself, such as one starting on a snow-covered ridgetop and descending into an arid desert environment, will only represent the total average for that line. Thus, the single-point average can be used to measure the average amount of water that will flow into a particular basin.

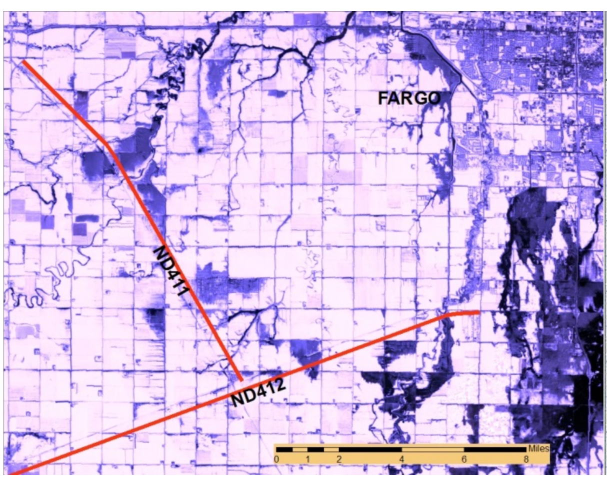

	A	B	C	D	E	F	G
1	LINE	K25	T25	GC25	SM	METHOD	DATE
1561	ND409	2849	865	29780	26.3	AI	101107
1562	ND410	3107	953	31120	24.8	AI	101107
1563	ND411	3105	1154	36780	26.4	AI	101107
1564	ND412	3064	1089	34800	26.5	AM	101108
1565	ND413	2453	757	27180	20	AM	101108
1566	ND414	2500	666	25670	27.7	AM	101108
1567	ND415	2999	961	32250	19.7	AM	101108
1568	ND416	2673	828	28620	24.7	AI	101107
1569	ND417	2289	520	22420	39	AM	101108
1570	ND418	3222	1054	33120	24.9	AM	101107
1571	ND419	2848	1015	34680	25.4	AM	101107

Figure 2. Flight lines ND411 and ND412. Both follow railroad tracks about 10 miles southwest of Fargo. On the right is the background data that is used to calculate the snow-water equivalent when the lines are flown in the winter.

```
: Total No. of flight lines sent = 10
:--------------------------------------------------------------------------------
:Line   Survey    %SC   SWE   SWE %SM Est Fall  %SM  Pilot
:No.    Date          (in) (35%) (M) Typ Date  (F)  Remarks
:================================================================================
LS120  DY160130 / 100 / 2.9 : 3.7, 52 151014     51 ,  0
LS132  DY160130 / 100 / 2.0 : 1.6, 27 151014     27 ,  0 frzn streams
LS333  DY160130 / 100 / 2.4 : 2.0, 28 151014     28 ,  0
LS365  DY160130 / 100 / 1.8 : 1.9, 36 151101     36 ,  0
WI111  DY160130 / 100 / 1.8 : 2.1, 42 151020     42 ,  0 open stream frzn lakes
WI112  DY160130 / 100 / 2.4 : 2.4, 35 151101     35 ,  0
WI113  DY160130 / 100 / 1.7 : 2.1, 43 151101     42 ,  0
WI114  DY160130 / 100 / 2.1 : 2.6, 44 151020     44 ,  0 frzn lakes
WI116  DY160130 / 100 / 2.1 : 2.4, 41 151020     41 ,  0 open streams frzn lakes
WI117  DY160130 / 100 / 1.2 : 1.7, 44 151101     44 ,  0
.END
Survey of northern Wisconsin and the shores of Lake Superior. Snow
observed on all lines. Lakes and rivers are frozen. Few streams are
open.
```

Figure 3. Standard Hydrometeorologic Exchange Format (SHEF) Message, including SWE measurements for each line flown that particular day, soil moisture values used in the SWE calculation, and pilot observations surrounding particular flight lines (Carroll 2001). SHEF messages are generated at the end of the survey day, processed, and posted at http://www.nohrsc.noaa.gov/snowsurvey/.

Airborne Survey Creation and Execution

Flight line data are collected as the principal component of an airborne snow survey in addition to photographs, videos, and pilot comments. Historically, most surveys contain about 50-150 lines and were flown within the span of about one to two weeks. The geospatial extent of each survey is usually within one River Forecast Center's domain, but they can vary in size from that of single small river basin, to an area the size of Alaska. Typical snow seasons have included anywhere between 10 and 20 individual surveys and an average of about 1000 flight lines. Historic airborne data are readily available from the National Weather Service at http://www.nohrsc.noaa.gov/snowsurvey/historical.html.

Surveys are created when a request is made from one of the NOAA River Forecast Centers to the Office of Water Prediction to collect airborne gamma data in their affected basins. Depending on conditions, river forecasters will make requests for specific flight lines, specific basins, general areas, or based on previous airborne surveys. The Principal Investigator for the program will then create a new survey based on the particular needs of the River Forecast Centers. The survey is then sent to the NOAA Corps pilots who are responsible for actually conducting the survey.

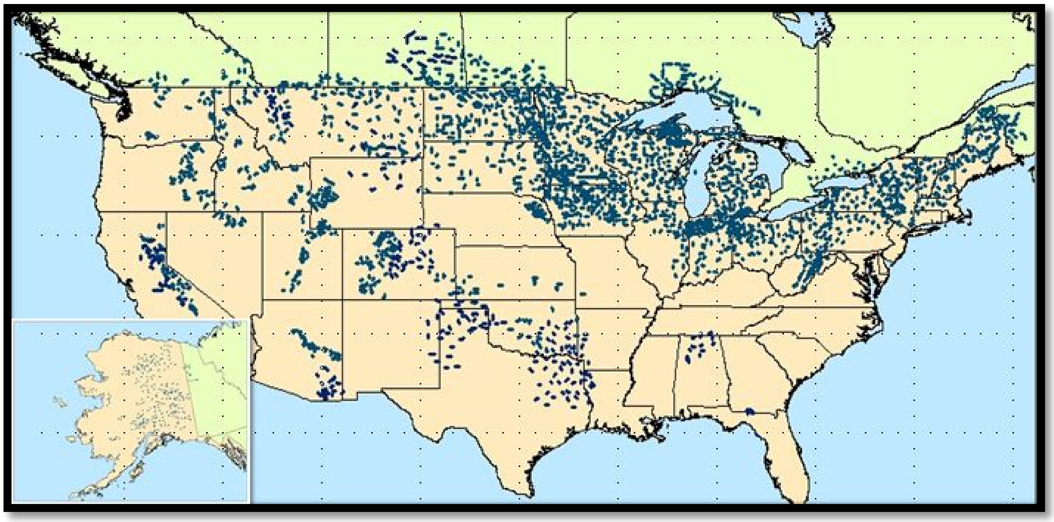

Figure 4. All 2600 flight lines available to the program as of Summer 2016.

The advantage of the airborne gamma detection survey is that it can cover a large area in a short amount of time. Surveys can generally be conducted quickly enough after a major snowfall event to cover an entire region before significant snowmelt occurs. However, there are the following constraints on the program:

1. Detection systems: As of Summer 2016, there are only two fully functional and calibrated sensor packages. More are available for future use, but are not currently useable because of the next constraint.
2. Aircraft: The aircraft that are used have to be engineered to be compatible with the sensors. Additionally, each aircraft has to be calibrated to account for its own unique gamma signature. Therefore, there are currently only three aircraft that are configured and calibrated to work with the two detection systems. The aircraft that are currently flown for the program require about 1-2 weeks of scheduled maintenance every two months, which can significantly hinder operations when only 2-3 aircraft are available in the first place. As a government asset, there is also competition with other programs within NOAA for aircraft availability.
3. Pilots/Personnel: Airborne gamma detection requires specific training and is only conducted by qualified NOAA Corps Aviators. Mission commanders typically take a full year to complete their qualifications.
4. Weather: Flight lines are flown at 500 feet above the ground, and require visual meteorological conditions (good weather) in order to safely conduct operations.

For these reasons, it is important to maximize the efficiency with which operations are conducted. Reducing the total number of flight lines for any given survey would reduce the flight time, cost, and duration of that survey, potentially freeing up the aircraft and crew to survey additional areas. The overall purpose of this project is to analyze the sampling efficiency of the program throughout its history and then to apply that analysis to develop a sampling framework for the program to use in the future.

Methods

Data Organization and Cleaning

The first step in the project was to organize the entire dataset into a single database that would allow for easy sorting and querying. The data set for the entire history of the airborne snow survey program is readily available at http://www.nohrsc.noaa.gov/snowsurvey/historical.html. The first 30 years of the data are available by decade, and contain the line number, date flown, and measured SWE value. Since this was all that was required, these records were downloaded and merged into a single spreadsheet.

The GIS dataset of interest was that of the NOHRSC flight lines, available at http://www.nohrsc.noaa.gov/gisdatasets/. The key piece of information in this data was the latitude and longitude of the midpoints for each flight line. Once downloaded, the database for the GIS dataset was merged with the historical dataset based on flight line name, such that the spreadsheet of the historical records contained the latitude and longitude of the midpoints of the flightline, which could then be used in the project analysis. Since this data contained over 25,000 unique flight line records, they would be suitable for the initial search for over-sampling potential. Data collected since 2010 was evaluated, but since it was sorted by survey and not decade, they were not added to the master histororical data set

Survey Selection

The purpose of the project was to investigate the potential for over-sampling, therefore finding an area with a high degree of sample volume was the most appropriate. One important aspect of the investigation was to remove as many factors for snow-water variability as possible. Therefore the focus area would be contained in a fairly limited geographic area (one or two states), have minimal terrain features, and the survey should occur over a short time period.

In order to limit temporal variation within the survey area, the simplest method proved to be in limiting the survey period to a single day. This method revealed that the highest survey day was 02 April 2009, on which 73 unique survey lines were collected. 84 lines in total were flown that day, 11 of which were repeated by overlapping aircraft (Figure 4).

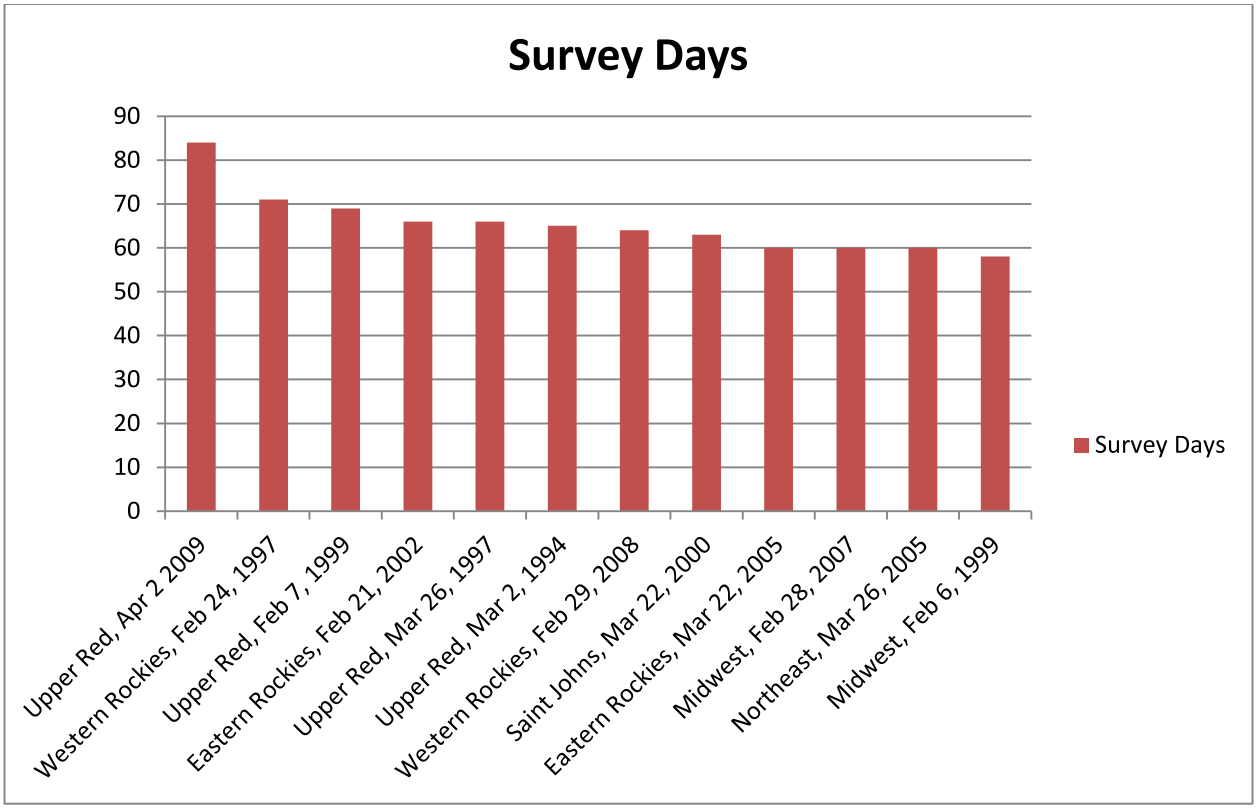

Figure 5. Total lines flown on highest collection days. The most productive survey day in the program's history in terms of total lines flown was April 2, 2009. Not included in this chart are the highest survey days since 2010, but there were no single days during that period that exceeded April 2, 2009.

The highest volume for a single day's output was April 2, 2009. This particular survey day met all the requirements, as most of the samples were near enough to each other that some degree of spatial autocorrelation could be assumed. With 73 lines covering approximately 70,000 square miles, this was also a relatively dense survey. The flat prairie of North Dakota would also limit other contributing factors to snow-water equivalent variability, such as slope, aspect, elevation, and temperature.

Since the lines were all flown on the same day, the only data fields of interest were the Flight Line Number and the SWE (in) representing the actual measured SWE. While there were 84 lines actually flown on that day, 11 of the lines were repeats by a second aircraft. The SWE measurements on the repeated lines were within 0.5 inches, and so an average value for each flight line was sufficient to use in the analysis.

NAME	LAT_MIDP	LON_MIDI	SWE
MB101	49.18865	-98.4322	3.6
MB102	49.26732	-98.7475	2.6
MB103	49.12398	-99.0672	2.7
MB104	49.12254	-99.6682	3
MN110	46.81181	-96.4953	2.1
MN111	46.52819	-96.4862	1.8
MN112	46.36227	-96.5491	2.9
MN123	46.61363	-96.7411	2.4
MN126	46.2772	-96.4198	2.3
MN127	46.32778	-96.4698	2.6
ND105	48.91382	-102.246	3.4
ND106	48.88915	-102.393	2.3
ND110	48.44448	-101.732	3
ND111	48.28152	-101.65	4.3
ND114	48.7597	-101.397	4
ND115	48.62617	-101.484	4.5
ND116	48.8015	-100.193	2.4
ND117	48.81629	-100.572	4.1
ND118	48.01216	-100.829	5.3
ND119	48.08414	-100.599	5.5
ND130	48.30827	-101.616	4.7
ND201	48.35909	-99.6039	4.5
ND202	48.63758	-99.5024	4.5
ND205	48.49204	-99.1188	3.4
ND206	48.90681	-98.9463	4
ND207	48.88831	-98.3564	3.1
ND210	48.69568	-98.1386	3.8
ND212	48.44969	-98.5024	3
ND213	48.18577	-98.366	4.2
ND222	47.69422	-99.9122	5.7
ND223	47.56596	-99.1103	5.4
ND226	47.87533	-97.9812	2.6
ND230	48.70146	-99.1897	4
ND231	48.39829	-98.8914	3
ND234	48.31475	-97.8532	2.2
ND236	47.52146	-97.8437	2.7
ND237	47.8104	-99.5045	5.4
ND240	48.53735	-98.6746	2.7
ND241	48.69835	-98.844	2.95
ND242	48.52317	-98.433	3.1
ND244	48.2861	-98.1259	3.5
ND245	47.92736	-99.7615	4.8
ND246	47.95138	-99.3684	5.1
ND307	47.13467	-101.792	3.3
ND310	46.99573	-100.529	3.7
ND321	46.86798	-101.599	3.6
ND401	47.47085	-99.5224	5.9
ND402	47.24901	-98.9806	4.9
ND404	47.23875	-97.6599	3
ND405	47.01887	-97.5627	3.3
ND410	46.52092	-98.3329	3.7
ND411	46.79329	-97.1322	5
ND412	46.70442	-97.0767	3.4
ND413	46.52794	-96.9125	1.7
ND414	46.33912	-97.2121	2.85
ND415	46.25593	-96.9743	2.7
ND416	46.75803	-97.5784	3.1
ND417	46.44879	-97.3971	3.1
ND423	46.70902	-98.7034	3.5
ND424	46.52484	-98.5799	3.6
ND427	46.39829	-97.795	2.6
ND430	46.32218	-96.9908	2.6
ND433	46.76996	-98.0902	3.5
ND434	46.84434	-97.877	3.6
ND435	46.6254	-97.7618	3.2
ND436	46.09433	-97.3425	1.9
ND437	46.20215	-97.142	2
ND439	46.20676	-96.8424	3.3
ND440	46.14494	-96.6261	3.1
ND442	46.00763	-96.6983	2.8
SK303	49.2201	-103.143	4.1
SK313	49.15366	-103.63	4.3
SK316	49.41261	-103.799	3.3

Figure 6. Snow-water equivalent data collected on April 2 2009, merged with the latitudes and longitudes of each flight line midpoint.

The data for April 2, 2009 was then copied into its own spreadsheet and saved as a comma-delimited file. The file was then opened in ArcMap, using the latitude and longitude of the midpoints as the X,Y coordinated, allowing for further spatial analysis. (Figure 8.)

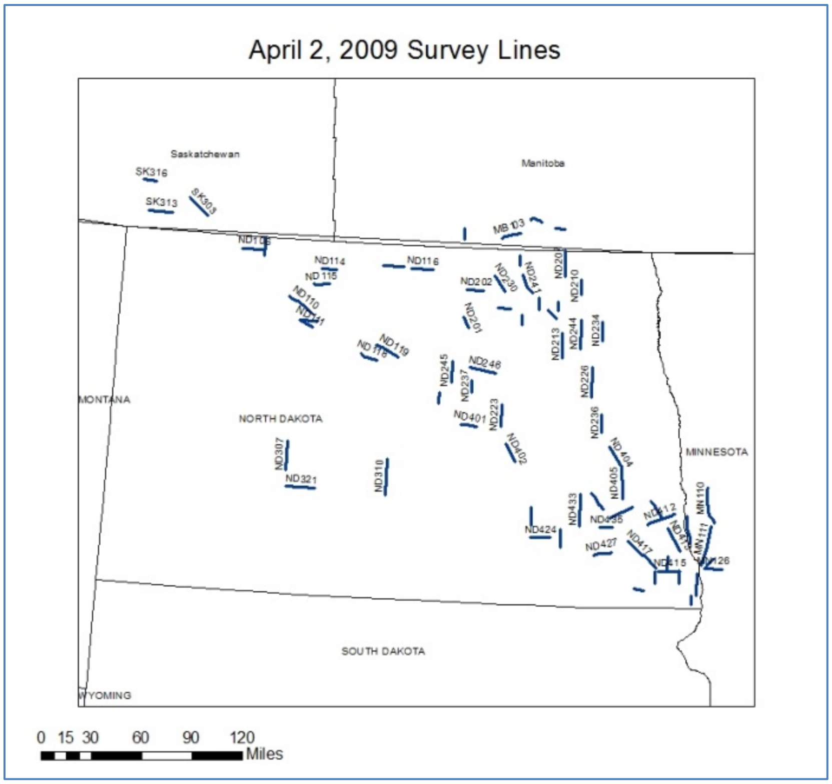

Figure 7. Flight Line Map of all lines flown on April 2,2009.

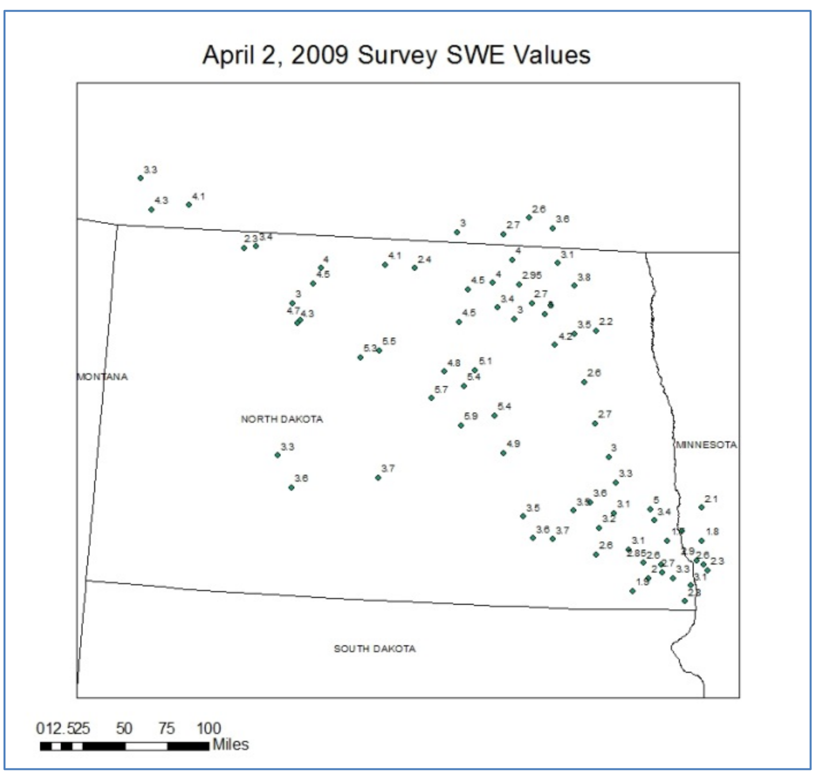

Figure 8. Snow-water equivalent values collected on April 2, 2009

Sample Optimization

The next step was to take the data from the candidate survey day, April 2 2009, and reduce the overall sample size in order to determine if fewer samples could still lead to an accurate snow-water-equivalent surface product. Four sample optimization strategies were used to examine how the sampling regime could be reduced, if at all. These included the random reduction, density dependent reduction, focused reduction and subjective reduction. For each method, the original sample of 73 lines was reduced by 5, 10, and 25%.

Optimization Strategy 1: Random Reduction: In order to randomly remove 4 samples from the original survey, the survey file for that day was opened in excel and each record was assigned a random number between 1 and 20. The four records with the highest random numbers were then deleted from the file and saved as "20090402Random95" to indicate 95 percent of the original survey. The same method was used for the 10 percent reduction and the 25 percent reduction. Each of these files was then opened in ArcMap as a table and converted to point shapefiles using the above methodology from the previous section. (Figure 9)

Optimization Strategy 2: Density Dependent Reduction: This strategy was based on the assumption that areas with higher densities of samples were the most likely to have been over-sampled. The result of this strategy would make the sampling density of the whole survey area appear more uniform. To reduce the number of samples by density, the first step was to create a kernel density raster, based on the spatial distribution of the points themselves. Then using the Extraction tool, the density at each sample point was extracted from the Kernel Density Raster. However, once a sample point was removed, it was understood that the point density would subsequently change. So this methodology had to be repeated for each point removal down to the 95, 90, and 75 percent level. As this would only have to be done once, the choice was made to accomplish this manually rather than attempt to automate the process (Figure 9)

Optimization Strategy 3: Focused Reduction: This strategy was based on the assumption that certain areas would have higher degrees of spatial autocorrelation than others, and that samples within those areas could be removed with little to no effect on the final product. This was done partially to test the theory that there was a high degree of spatial autocorrelation among the flight lines that were near to each other. To do this, a Cluster and Outlier Analysis was conducted, applying an Anselin Local Moran's I to each feature. Feature points with high local Moran's I values would be removed from the survey. Similar to how the Density Optimization method was applied, this had to be an iterative approach. Simply removing all the features with the highest spatial autocorrelation index would result in the removal of an entire cluster, which was something to be avoided. As there were only two clusters evident in the data, one high and one low, a point feature was removed each time. In order to remove a feature based on spatial autocorrelation index, the p-value for that index was also looked at, and only features with p-values less than .05 were removed (Figure 9)

Optimization Strategy 4: Subjective Analysis: This strategy was based on the original premise that some lines simply appeared to add little value to the overall model due to their limited variation from nearby lines. Through a visual analysis of the points along with their values, lines were removed in the same manner, but not using any defined methodology.

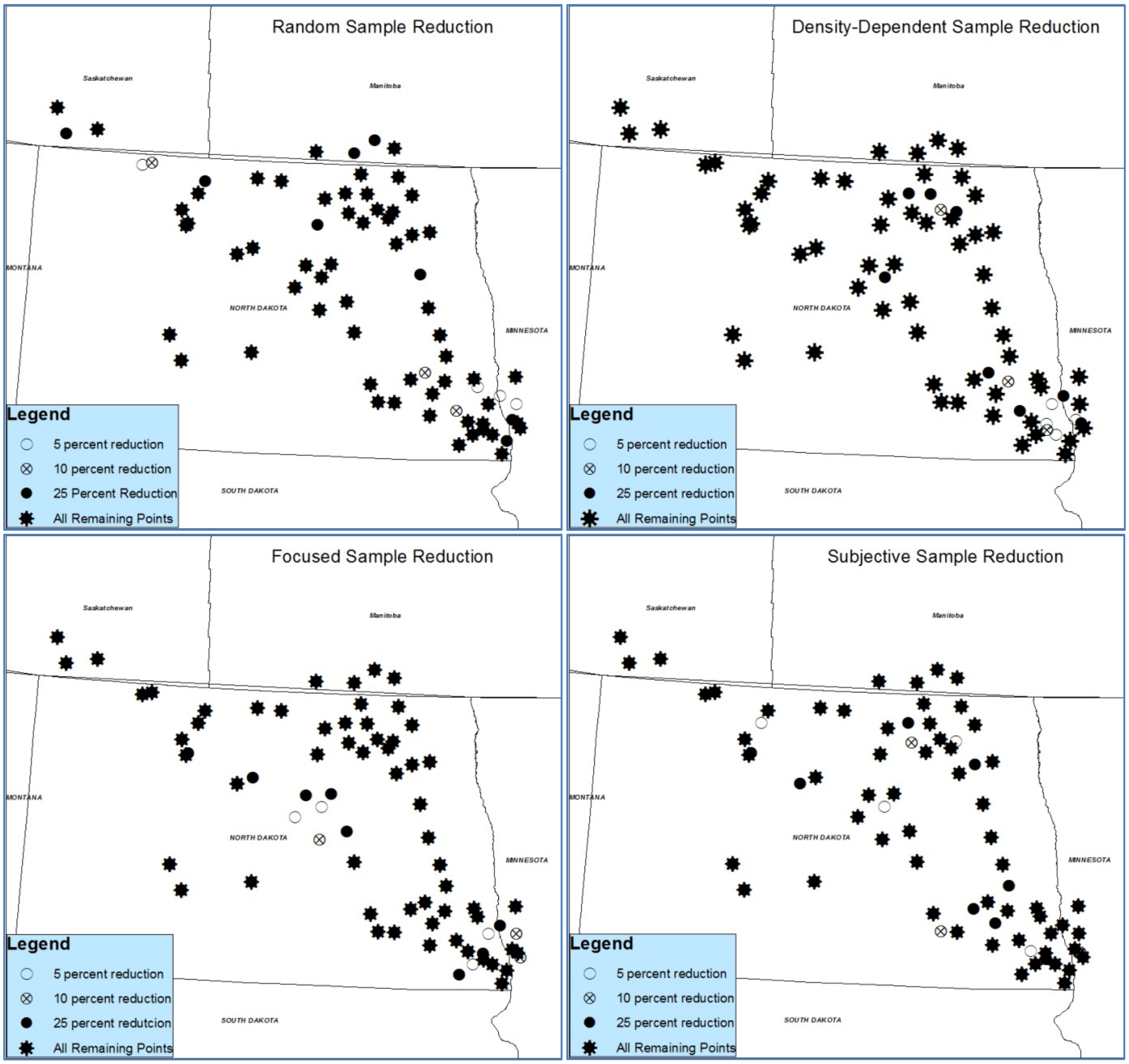

Figure 9. Sampling optimization. Open circles represent the samples removed from the 5 percent reduction, crossed-circles represent additional lines removed during the 10 percent reduction, and solid circles represent the additional lines removed by the 25 percent reduction.

INTERPOLATION OF REMAINING SAMPLES

The next step in the process was to create an interpolated surface based on the remaining samples following the optimization. Several different interpolation methods were utilized, but the two methods that proved the most reliable with creating realistic snow-water-equivalent surfaces were Inverse-Distance-Weighted (IDW), and Kriging. Both methods were used on each optimized sample in order to determine which method gave consistently lower sample errors.

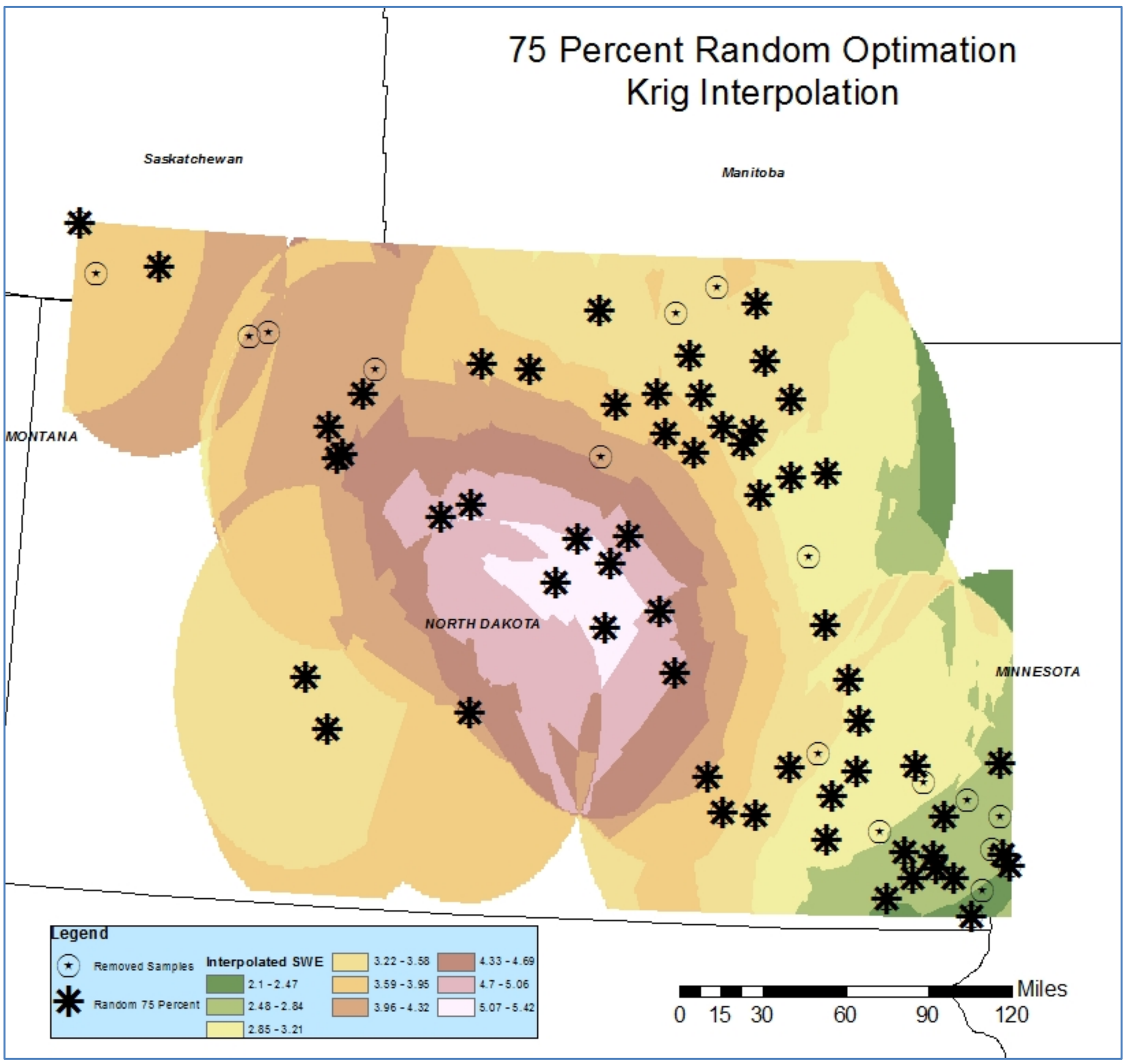

Figure 10. Interpolated surface of the randomly optimized 75 percent sample using Kriging.

EXTRACTION FROM INTERPOLATED SURFACES

The next step was to extract the results from the interpolated surfaces onto the samples that were removed from the original sample. This was accomplished using ArcTools Extract from Grid Tool on the

the interpolated surface and the removed samples. The interpolated values were then stored within the data for the removed samples.

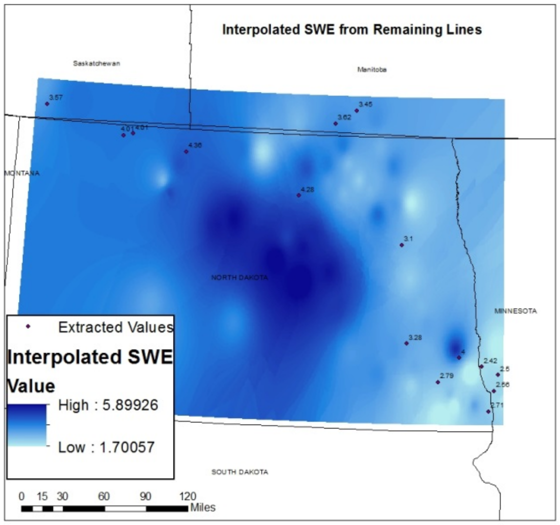

Table

Rand25_output

NAME	ELEV_FT	LAT_MIDPNT	LON_MIDPNT	SWE	rando	IDW_SWE
ND412	915	46.704421	-97.076658	3.4	100	4
ND106	1939	48.889153	-102.392587	2.3	99	4.01
MN123	915	46.613626	-96.74112	2.4	99	2.42
MN111	968	46.528187	-96.48617	1.8	99	2.5
ND105	1909	48.913817	-102.246082	3.4	98	4.01
ND434	1391	46.84434	-97.877026	3.6	97	3.28
ND417	1073	46.44879	-97.397074	3.1	95	2.79
MB102	1440	49.267321	-98.747507	2.6	91	3.45
MB103	1503	49.123978	-99.067169	2.7	91	3.62
ND114	1575	48.759696	-101.396769	4	91	4.36
SK313	1946	49.153663	-103.629961	4.3	91	3.57
ND201	1631	48.359093	-99.603912	4.5	91	4.28
ND440	961	46.144936	-96.626121	3.1	89	2.71
MN112	958	46.362269	-96.549065	2.9	86	2.56
ND226	1490	47.875328	-97.981234	2.6	86	3.1

0 (0 out of 15 Selected)

Rand25_output

Figure 11. Extraction of Interpolated SWE values into the removed sample flight lines for the 25 percent random reduction. Note that the table on the left contains both the originally measured SWE value and the interpolated SWE value (IDW_SWE).

SAMPLE ERROR CALCULATION

The final step in the analysis was to calculate the sample error between the interpolated values and the original measurements within the removed samples. This was accomplished by using the Standard Deviation function in Excel.

F	G	H	I	J	K	L	M	N
NAME	ELEV_FT	LAT_MIDPNT	LON_MIDPNT	SWE	random	Inter_SWE	Error (InterSWE-SWE)	
ND412	915	46.70442093640	-97.07665774310	3.40000000000	100	3.99965858459	0.59965858459	
ND106	1939	48.88915309480	-102.39258744100	2.30000000000	99	4.01117229462	1.71117229462	
MN123	915	46.61362623300	-96.74111976550	2.40000000000	99	2.41969919205	0.01969919205	
MN111	968	46.52818712010	-96.48616951920	1.80000000000	99	2.49825453758	0.69825453758	
ND105	1909	48.91381716580	-102.24608241400	3.40000000000	98	4.01129531860	0.61129531860	
ND434	1391	46.84433968290	-97.87702622620	3.60000000000	97	3.27522349358	-0.32477650642	
ND417	1073	46.44878980670	-97.39707365980	3.10000000000	95	2.79006004333	-0.30993995667	
MB102	1440	49.26732064630	-98.74750682560	2.60000000000	91	3.44538807869	0.84538807869	
MB103	1503	49.12397831870	-99.06716857080	2.70000000000	91	3.61531877518	0.91531877518	
ND114	1575	48.75969635550	-101.39676937600	4.00000000000	91	4.36221122742	0.36221122742	
SK313	1946	49.15366330900	-103.62996072100	4.30000000000	91	3.57177877426	-0.72822122574	
ND201	1631	48.35909298450	-99.60391153770	4.50000000000	91	4.28274822235	-0.21725177765	
ND440	961	46.14493622190	-96.62612148720	3.10000000000	89	2.70775723457	-0.39224276543	
MN112	958	46.36226871410	-96.54906475140	2.90000000000	86	2.55510091782	-0.34489908218	
ND226	1490	47.87532755440	-97.98123369590	2.60000000000	86	3.09501314163	0.49501314163	
							0.63742439455	Sample Error in Inches

Figure 11. Sample Error Calculation for the random 25 percent reduction with IDW interpolation. The average amount in the lower right represented the sample error result for that particular method of optimization and interpolation.

SAMPLE ERROR RESULTS

Using the above methodology, sample errors were calculated for each optimization strategy and interpolation method combination (Figure 12). The original data was recorded in standard units, but the sample errors were converted to metric for analysis of the results.

Optimization	Percentage	Remaining Samples	Extracted Samples	Interpolation Method	Sample Error (CM)
Random	95	69	4	IDW	0.99
Random	95	69	4	Krig	1.85
Random	90	66	7	IDW	1.7
Random	90	66	7	Krig	1.45
Random	75	58	15	IDW	1.63
Random	75	58	15	Krig	1.73
Density	95	69	4	IDW	1.7
Density	95	69	4	Krig	1.08
Density	90	66	7	IDW	1.4
Density	90	66	7	Krig	1.5
Density	75	58	15	IDW	1.24
Density	75	58	15	Krig	1.23
Focused	95	69	4	IDW	1.93
Focused	95	69	4	Krig	1.73
Focused	90	66	7	IDW	2.06
Focused	90	66	7	Krig	2.16
Focused	75	58	15	IDW	2.44
Focused	75	58	15	Krig	2.44
Subjective	95	69	4	IDW	0.51
Subjective	95	69	4	Krig	0.69
Subjective	90	66	7	IDW	0.58
Subjective	90	66	7	Krig	0.76
Subjective	75	58	15	IDW	0.51
Subjective	75	58	15	Krig	0.86

Figure 12. Summary of sample error results from different optimization strategies and interpolation methods.

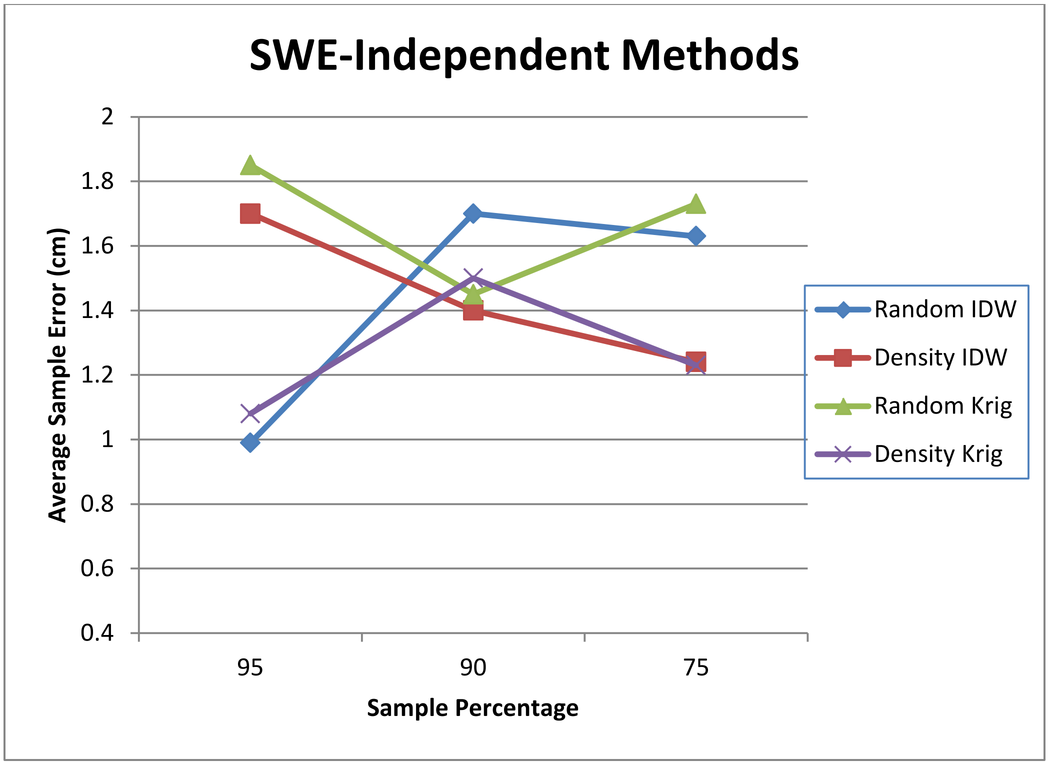

Figure 13. Results for SWE-independent optimization strategies

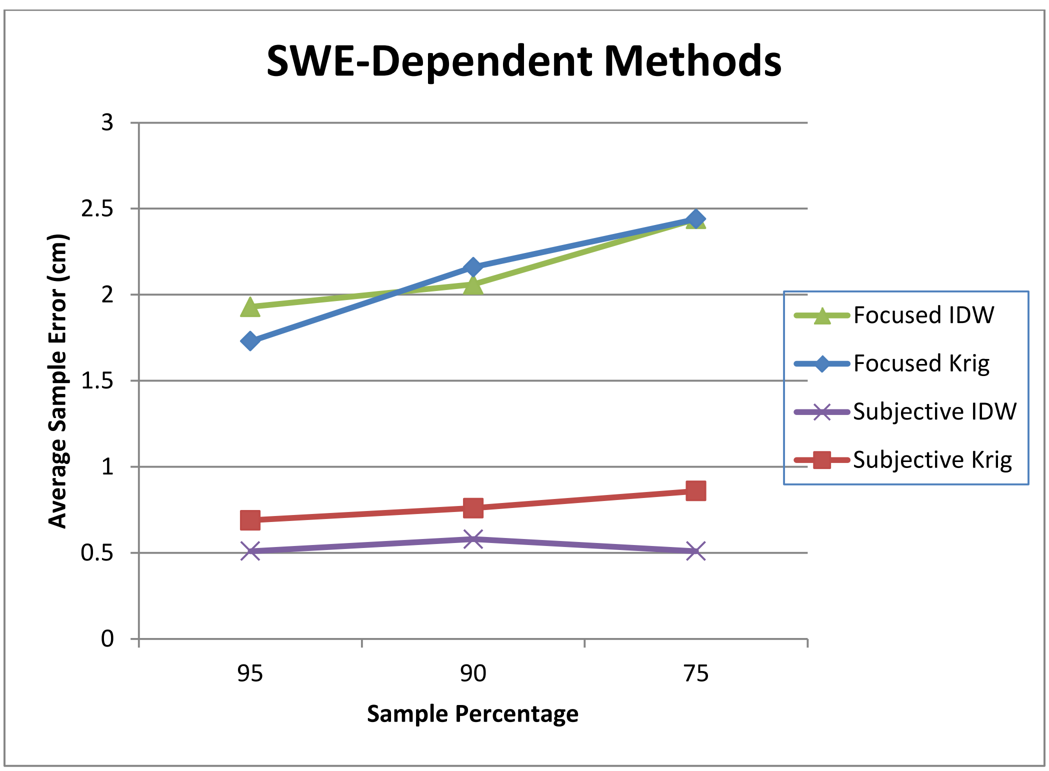

Figure 14. Results for SWE-dependent of each optimization strategy.

Discussion

For the purposes of this analysis, an average sample error of 1 cm represented the acceptable error for any optimization strategy or interpolation method. However, the acceptable sample error in the operational environment of the airborne program would ultimately rely on the requirements for that particular survey. A survey like the one conducted on April 2, 2009 would have very strict accuracy requirements, due to the immediate impact of snowmelt on the metropolitan areas of Fargo and Grand Forks. A survey in the mountains of Colorado would likely have a much higher acceptable error, based on the highly variable nature of the snowpack in the mountains. The average sample error ranged from a low of 0.99 cm for the random 95 percent optimization to a high of 2.44 cm on the focused 75 percent optimization. Individual sample interpolation errors ranged from up to 5 cm low to 5 cm cm high.

SWE-dependent versus SWE-independent optimization strategies: There were two basic optimization strategies employed in this analysis. The SWE-independent methods were capable of being applied to any survey area and did not rely on the SWE measurements themselves. The SWE-dependent methods were based on the theory that snow-water equivalent measurements would consistently demonstrate a measureable amount of spatial autocorrelation. These methods would not be useful in creating more efficient surveys, but they could be used to demonstrate the existence and level of spatial autocorrelation, as well as whether any other input parameters could be in play.

Random optimization strategy: Extracted average sample error would normally be expected to increase as the original sample percentage went down, but this pattern was not observed for either of the interpolation methods of the randomly optimized sample. Furthermore, the difference between 95 and 90 percent reduction was only 3 flight lines, magnifying the effect that one outlying line could have on the overall accuracy of the method. However, the IDW-interpolation of the 95 percent randomly optimized sample was the only SWE-independent method that resulted in an acceptable sample error (0.99 cm).

Density Dependent Optimization strategy: The density-dependent optimization strategies would have also been expected to follow a pattern of increased sample error as more samples were removed. As with the random strategy, this did not prove to be the case. Interesting, at the 75 percent optimization level, the average sample error crept back down from the 90 percent level.

Focused Optimization Strategy: The focused optimization strategy resulted in the highest sample error of any of the optimization strategies. This was something of a surprise, considering that the method used a local cluster analysis to remove samples that demonstrated the strongest relationship with nearby samples. There are several potential reasons for this which could be tested. One would be that removing the samples with the highest spatial autocorrelation actually removes critical values that would prove to be more useful in an interpolation and not less. Another reason could be that the parameters for local neighbors was either too wide or too narrow. However, the sample error did steadily increase as more samples were removed, which was in line with expectations.

Subjective Optimization Strategy: With sample errors between 0.5 and 1.0 cm, the subjective strategy did indeed prove the idea that some lines could be interpolated effectively without being flown. The problem with this strategy, like the focused optimization strategy, was that it is SWE-dependent, so there is no way to know which lines those would be until they were flown. Further analysis could be conducted to determine if any specific flight lines consistently demonstrated high degrees of spatial autocorrelation. If so, they would be candidates for permanent removal from the flight line database.

Testing of Method on Another Survey

The next highest survey day for the area was Feb 2, 1999.This survey had almost no overlap with the one from Apr 2, 2009, so another high sample survey day was chosen, March 2, 1994.To determine whether or not the sample error values collected from the previous section would hold the same for other surveys in a nearby location, the density-dependent optimization strategy was tested on another similar survey. This method was applied to data collected on Mar 2, 1994, which shared a similar geographic distribution and many common flight lines with Apr 2, 2009 (Figure 15), although it was a month earlier in the season. Most importantly, this survey also contained a relatively high number of samples, with 63 unique survey lines flown that day. The density-dependent optimization strategy was used to reduce the overall sample density from 63 to 58 samples, representing an 8 percent reduction.

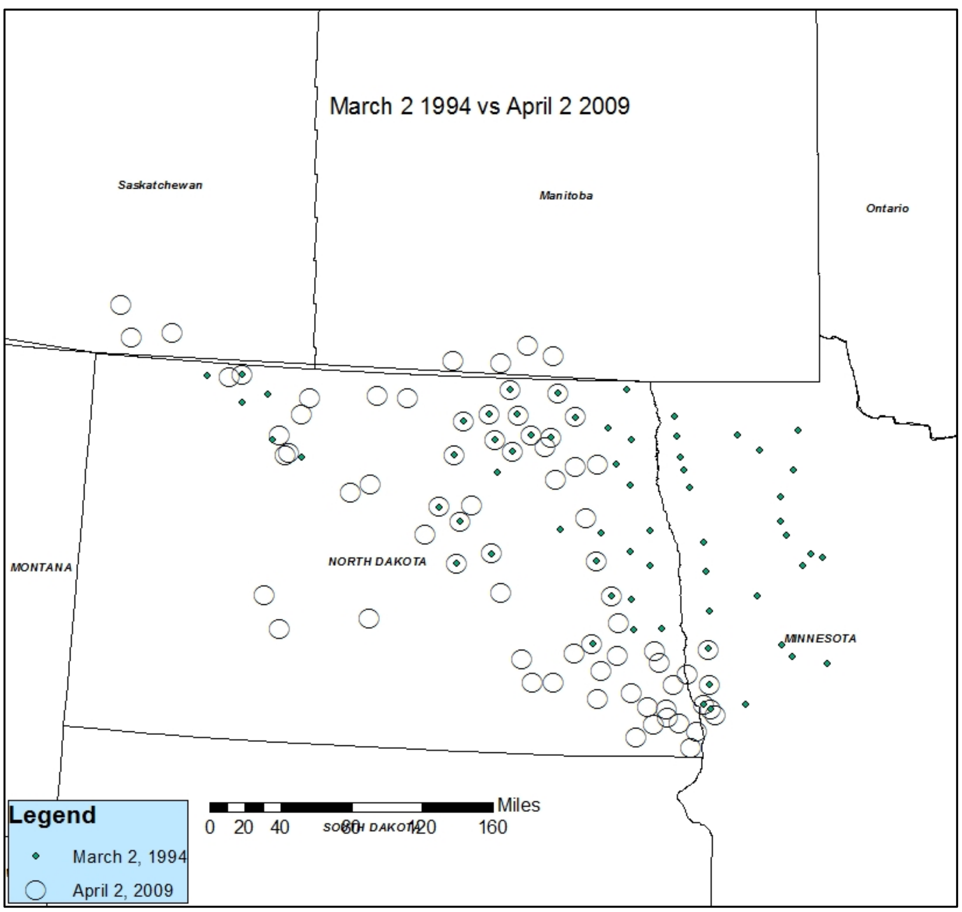

Figure 15. Survey flown on March 2, 1994 compared to survey flown on April 2, 2009.

The average sample error scores were even higher than they were for the 2009 survey, with a sample error of 4.14 cm for the IDW interpolation and 4.34 for the Krig interpolation. As was seen in the analysis of the sample error in the candidate survey, a handful of outlying sample values significantly skewed the results of the second survey analysis.

Conclusions

This study involved sorting through 35 years of historical airborne snow-water equivalent surveys to determine whether or not the highest density surveys represented any tendencies towards over-sampling. If any over-sampling were found, then the methods used in this study could be utilized on other surveys in order to maximize the efficiency at which these critical government assets are deployed. The specific survey day that was chosen for analysis was April 2, 2009, with data on 73 individual flight lines collected. Two methods of variable-independent sample optimization were used, random and highest density. Two methods of variable-dependent sample optimization were also used, spatial autocorrelation analysis and subjective sample removal. The results from this analysis yielded unacceptably high average sample errors for the first 3 methods. The low sample error in the subjective analysis helped to demonstrate the degree of spatial autocorrelation that could only be seen after the fact, and on lines that were very near each other.

While the average sample errors were outside of the accuracy tolerance for this project, there remains plenty of research to be conducted within the historical data set that could be used to improve operational efficiency. Individual flight line analysis was outside the scope of this project, but there exists the possibility that certain flight lines may demonstrate a historical tendency to closely match their nearest neighbors, and this may contribute little to the overall snow-water equivalent picture. This project tended to focus on the macro- or survey-level amounts variability of snow-water equivalent. Perhaps a more localized focus would yield different results.

As the need for snow-water equivalent data is gain importance in the future, it remains imperative to evaluate best practices for efficient data collection and allocation of government resources.

References

Adams, R.M., Houston, L.L, Weiher, R.F. 2004. The Value of Snow and Information Services. Report prepared for National Operational Hydrologic and Remote Sensing Center. http://www.nohrsc.noaa.gov/technology/pdf/NOAAs_National_Snow_Analyses.pdf accessed 11 Dec 2016.

Bales, R.C., Cline, D. 2016. Snow Hydrology and Resources Western United States. http://www.climate-policy-watcher.org/hydrology/snow-hydrology-and-water-resources-western-united-states.html accessed 18 Nov 2016.

Carroll, T. 2001. Airborne Gamma Radiation Snow Survey Program: A User's Guide. Version 5.0 http://www.nohrsc.noaa.gov/special/tom/gamma50.pdf

Jones, W.K, Carroll, T.R. 1983, Error analysis of airborne gamma radiation soil moisture measurements. *Agriculture Meteorology*. Jones and Carroll 1983, v28, 19-30.

Moes, P. 2011. Digging up snow helps flood predictions. *Crosscurrents.* Vol 37, No 3. P3.

Todhunter, P.E. 2001. A hydroclimatological analysis of the Red River of the North Snowmelt Flood Catastrophe of 1997. *American Water Resources Association* 37(5). p 1263

United States Army Corps of Engineers. 1992. Airborne Remote Sensing. *Great Lakes Levels- May 1992 http://www.lre.usace.army.mil/Portals/69/docs/GreatLakesInfo/docs/UpdateArticles/Update082.pdf.* Accessed 18 Nov 2016.